

# Nutrient limitation of microbial phototrophs on a debris-covered glacier



J.L. Darcy, S.K. Schmidt\*

Department of Ecology and Evolutionary Biology, University of Colorado, Boulder, CO, 80309, USA

## ARTICLE INFO

### Article history:

Received 29 May 2015

Received in revised form

29 December 2015

Accepted 29 December 2015

Available online 13 January 2016

### Keywords:

Nitrogen

Phosphorus

Alaska

Denali

Supraglacial debris

Microbial eukaryotes

## ABSTRACT

Photosynthetic microbial communities are important to the functioning of early successional ecosystems, but we know very little about the factors that limit the growth of these communities, especially in remote glacial and periglacial environments. The goal of the present study was to gain insight into the degree to which nutrients limit the growth of photosynthetic microbes in sediments from the surface of the Toklat Glacier in central Alaska. Previous studies and historical observations indicated that this environment is dominated by unique soil algae, and that succession from a microbial to a plant-dominated system is very slow. We used a soil microcosm approach to determine if nitrogen (N) and/or phosphorus (P) additions would affect the development and final biomass of microbial phototroph communities in this system. We found that fertilization with P significantly increased the exponential growth rate ( $r$ ), but P alone did not affect the final percent soil cover ( $K$ ) by microbial phototrophs. Nitrogen alone had no effect on either  $r$  or  $K$ , but the combination of P and N dramatically increased  $K$ , thus showing that algal growth rate in this system is likely P-limited, but total productivity may be co-limited by P and N. In addition, nutrient treatments differentially stimulated microbial groups resulting in significantly different microbial communities among treatments. Overall, these results give a preliminary indication of the factors that might limit the development and productivity of photosynthetic microbial communities in an extreme and remote glacial system.

© 2016 Elsevier Ltd. All rights reserved.

## 1. Introduction

Very few studies have examined nutrient limitation of photosynthetic community development in plant-free periglacial and glacial environments (Schmidt et al., 2012). The development of photosynthetic microbial communities is a critical early step in primary succession, contributing to soil formation that in turn is necessary for the establishment of macroscopic plant communities (Belnap and Lange, 2001, Nemergut et al., 2007). Schmidt et al. (2012) observed that in the glacial forelands of the Puca glacier in Perú, the development of photosynthetic crust communities was limited by phosphorus availability. However, this limitation may or may not be exclusive to that site or to the Peruvian Andes. Other environments in the cryosphere may impose different limitations on the development of microbial phototroph communities,

especially since cold desert environments differ in important biogeochemical factors (Schmidt et al., 2011a).

One type of cold desert environment that has received very little study are debris-covered glaciers, which are very common and extensive in terms of geographic coverage, especially in active geological areas such as the Himalayas and Alaska Range (Nakawo et al., 2000; Scherler et al., 2011). This environment is characterized by a thin layer of mineral debris on top of glacial ice, which is deposited allocthonously from the glacier's surroundings. One such glacier is the Middle Fork Toklat Glacier in the Alaskan interior (Alaska Range) which is covered with oligotrophic mineral soils, is not colonized by plants (Schmidt and Darcy, 2014), and is located in Denali National Park and Preserve, which has very low rates of nitrogen deposition (Fenn et al., 2003). Before the present study, no work had been done on microbial phototrophs and nutrient limitation in the extreme environment atop debris-covered glaciers. However, nutrient limitation has been observed in heterotrophic microbial communities in several early-succession cold desert biomes. P limitation was observed for heterotrophic microbes of periglacial soils in the Colorado Rocky Mountains (King et al., 2008) and Peruvian Andes (Schmidt et al., 2011b), while N limitation

\* Corresponding author. Department of Ecology and Evolutionary Biology, Campus Box 334, Boulder, CO, 80309, USA. Tel.: +1 303 492 6248.

E-mail address: [Steve.Schmidt@Colorado.edu](mailto:Steve.Schmidt@Colorado.edu) (S.K. Schmidt).

(after C limitation was alleviated) was observed in the Swiss Alps (Göransson et al., 2011). However, nutrient limitations of heterotrophic communities may not translate to their co-occurring phototroph communities since microbial phototrophs may have access to different pools of P than their heterotrophic counterparts (Cleveland and Liptzin, 2007).

Although there has been much previous work on nutrient limitation and microbiology of cold-desert environments (King et al., 2008; Göransson et al., 2011; Schmidt et al., 2011b, 2012; Knelman et al., 2014), most of it has focused on recently deglaciated landscapes. However, except for the current study, work on supraglacial nutrient limitation has been limited to cryoconite holes (Stibal et al., 2009), which are substantially different from the soil-like surface of the Toklat Glacier. Cryoconite holes form when small amounts of debris are warmed by solar radiation and melt into the ice forming enclosed micro-communities. Although this process may happen in places atop the Toklat glacier, the supraglacial debris layer is over 20 cm thick, enough so that the ice beneath the debris cannot be seen. Microbiological studies of supraglacial debris are rare, with only two studies focusing on bacteria atop debris-covered glaciers (Darcy et al., 2011; Franzetti et al., 2013). Unsurprisingly, culture-independent studies of microscopic eukaryotes in supraglacial debris are even rarer yet, with the only currently published work being our previous study of unique algal clades on the Toklat Glacier (Schmidt and Darcy, 2014).

Here, we use a microcosm experiment, biogeochemical analysis, and culture-independent molecular methods to better understand the extreme supraglacial environment, and the role nutrient limitation may play in limiting microbial growth on top of a debris-covered glacier. To measure nutrient limitation, we employed and improved upon recently developed microcosm-based experimental protocols for comparing the degree to which common limiting nutrients (N and P) influence the growth of diminutive photosynthetic communities (Schmidt et al., 2012). We have taken this approach a step farther by phylogenetically characterizing the microbial communities from these microcosms to better understand selection processes that occur under different nutrient limitation conditions, and how they relate to organisms that may be found *in situ*. Together, our results form a detailed glimpse of phototrophic life in this harsh environment, and provide new insights into how different cryospheric bacteria and microbial eukaryotes may be affected by nutrient limitation.

## 2. Methods

### 2.1. Nutrient addition experiment

Microcosm plates were created using homogenized soil samples collected from atop the Toklat Glacier by Darcy et al. (2011). Homogenization was used to ensure that starting communities were similar among microcosms, and also representative of the organisms found *in situ*. A total of 20 microcosms were made, each consisting of 13 g of soil added to a 55 mm diameter Petri dish (Fisher Scientific 8-757-13A), sealed with Parafilm (Pechiney Plastic Packaging, Menasha WI, USA). Treatments consisted of a control (no nutrient addition), +N, +P, and +N+P. For each treatment, 75  $\mu\text{g}$  of N (as  $\text{NH}_4\text{NO}_3$ ), P (as  $\text{KH}_2\text{PO}_4$ ), or both were added (in aqueous solution) per gram of soil. All soils were initially amended to 70% of water holding capacity as described elsewhere (Schmidt et al., 2011b, 2012). Water holding capacity averaged 29% of dry weight across microcosms, therefore aqueous concentration was approximately 370  $\mu\text{g}$  of N and/or P per ml of water. Preliminary experiments indicated that these concentrations were high enough to overcome nutrient limitations in calcareous, early successional soils (Schmidt et al., 2011b, 2012). Microcosms were incubated at

21 °C under 16 h of light per 24 h, conditions that approximately mimic the relatively mild summer conditions at the toe of the Toklat Glacier (unpublished data). The arrangement of the plates was randomized every three days to account for any variation in light and temperature. Microcosms were surveyed twice weekly for coverage of microbial phototrophs using the field of view (FOV) method described by Schmidt et al. (2012), for a total of 15 time points over 51 days. When FOV measurements began to saturate (plateau), a variation of the point-intercept method was used instead, where a reticule was placed on the microscope's objective. Instead of counting a 'hit' when a photosynthetic colony was within the field of view, a 'hit' was counted when the cross-hairs (a single point) of the reticule intersected any photosynthetic organism or structure. This method was much more time consuming, but allowed for more accurate estimates of percent cover. Both types of measurement (FOV and point-intercept) were used in conjunction for several measurement periods before the FOV measurements began to reach saturation at day 34.

### 2.2. In-silico methodological validation

To correlate the two methods, an *in-silico* microcosm experiment was run (R code available upon request), which used both the FOV and point-intercept methods on randomly generated microcosm plates. To ensure a broad distribution of covers across generated microcosm plates, plates were generated with preset naïve covers ranging from 0 to 80% cover, calculated by the total area of all colonies divided by the total area of the plate. This naïve cover is inaccurate by design because of overlap between colonies, however it was only used to ensure a wide range of actual *in silico* covers (as estimated by percent cover) for correlative purposes. We also confirmed that the *in-silico* point-intercept method is highly accurate, by using Adobe Photoshop's (Adobe Inc., San Jose CA, USA) magic wand tool to calculate the ratio of green pixels to white pixels on graphical representations of the *in-silico* microcosms (Supplemental Fig. 1, first panel). The trend between FOV and point-intercept data observed in the *in-silico* experiment was best modeled using a general 1-parameter exponential decay model (Equation (1)) (Supplemental Fig. 1, second panel), which was fit to the observed data using the Gauss-Newton algorithm in R 3.0.2 (R Core Team, 2013) (Supplemental Fig. 1, third panel). This model was then used to convert real FOV data from before day 34 of the microcosm experiment to percent cover estimates.

Equation (1): Exponential decay.

$$f(x) = 1 - e^{-Ax} \quad (1)$$

### 2.3. Growth curve modeling and statistical analysis

Time series of percent cover data for each of the 20 microcosms were modeled using the general logistic growth function (Equation (2)) in R using the Gauss-Newton algorithm. The logistic growth function we used has been described elsewhere (e.g. Schmidt et al., 2011b) and models growth as a function of time ( $t$ , days), with three parameters: The upper asymptote ( $K$ , final percent cover), the exponential growth rate ( $r$ ,  $\text{days}^{-1}$ ), and the position of the inflection point ( $i$ , days). The point on the logistic curve where  $t = i$  has the steepest instantaneous growth rate (i.e. % cover gained per day). In this version of the logistic equation, the lower asymptote is fixed at zero. Fit parameter values for each nonlinear model were used in three 2-way ANOVAs with interaction to test for the effects of N and P addition on growth response, using Boolean independent variables for N and P.

Equation (2): Logistic growth.

$$f(t) = K / (1 + e^{-r(t-i)}) \quad (2)$$

#### 2.4. Microcosm biogeochemical analysis

Microcosms were destructively sampled after the microcosm experiment to determine residual concentrations of nitrate, nitrite and ammonia. Five grams of soil from each sample were combined with 25 ml 0.5 M K<sub>2</sub>SO<sub>4</sub> and shaken at 150 rpm for 1 h, then centrifuged for 1 h at 4000 rpm. This same procedure was carried out on a “blank” sample containing no soil. Dissolved nitrate+nitrite concentrations for each sample (including the blank) were analyzed using a Lachat QuickChem 8500 (Hach Ltd, Loveland CO, USA) and dissolved ammonia was analyzed colorimetrically using a BioTek Synergy 2 microplate reader (BioTek, Winooski VT, USA). Nitrogen (N) concentrations were back-calculated stoichiometrically and corrected for background N levels using the blank sample data. Corrected values were tested for a difference among treatments using Tukey's HSD test.

#### 2.5. High-throughput 16S and 18S rDNA sequencing

After the microcosm experiment, genomic DNA was extracted from 3 replicate microcosms of each treatment (12 total) using the MoBio PowerSoil kit (Carlsbad, CA, USA). Each extraction was amplified in triplicate using the bacterial primer set 515F/806R (Caporaso et al., 2012) and the eukaryal primer set 1391f/EukBr (Amaral-Zettler et al., 2009). Each primer oligo included an Illumina flowcell adapter, and different GoLay barcodes were used for each of the 12 samples and 2 genes (16S and 18S), for a total of 24 barcodes. Both primer sets are from the Earth Microbiome Project standard protocols (accessible at <http://press.igsb.anl.gov/earthmicrobiome/emp-standard-protocols>). Each set of triplicate reactions was pooled, and amplicon concentrations were assayed using Pico Green fluometry on a BioTek Synergy 2 microplate reader (BioTek, Winooski VT, USA). Amplicons were diluted to equimolar concentration, pooled, and sequenced on the Illumina MiSeq platform (Illumina, Inc.) using paired-end 2 × 150bp chemistry. A 30% phiX spike was added to the run to compensate for the otherwise limited amplicon variability (Caporaso et al., 2012).

#### 2.6. Bacterial and eukaryal community analysis

Raw reads were demultiplexed and quality filtered using QIIME (Caporaso et al., 2010). For bacterial reads, paired-end sequences were joined. However, this process did not work for eukaryal reads, so only the read corresponding to the 1391F primer was used. This read was selected instead of its pair because a sequence closer to the center of the 18S gene overlaps more with the majority of sequences in the NCBI and SILVA databases, allowing for better taxonomic assignment. Both the bacterial and eukaryal data sets were separately clustered at 97% sequence similarity using UCLUST (Edgar, 2010), and taxonomy was assigned using QIIME's parallel\_assign\_taxonomy\_blast.py script and the SILVA Ref NR 99 database's taxonomic information. When this method was not sufficient for classification of an abundant OTU (>2% community composition) to the genus level because it returned “unclassified”, BLAST (Altschul et al., 1990) was used with the NCBI Nucleotide database to find a close match, cultured or otherwise. Using this taxonomic information, all mitochondrial and chloroplast OTUs were removed from the bacterial data set, and all bacterial OTUs were removed from the eukaryal data set. Both data sets were then rarefied to the number of sequences equal to their least populous

sample. The bacterial data set was rarefied to 19000 sequences per sample, and the eukaryal data set was rarefied to 5000 sequences per sample. Weighted UniFrac (Lozupone and Knight, 2005) was used to compute beta-diversity matrices for both data sets, which were tested for the influence of N and P using ADONIS from the R package vegan (Oksanen et al., 2013) with Boolean independent variables for N and P. Principal coordinate analysis was used to visualize these data. Alpha rarefaction was performed in QIIME using the rarefied eukaryal data set with both the species observed and Faith's (1992) phylogenetic metrics. Phylogenetic trees were constructed for each data set, since UniFrac and Faith's (1992) phylogenetic metrics are both phylogenetic metrics, and require trees as input. Bacterial and eukaryal representative sequence sets were each aligned to reference using the SINA aligner (Preusse et al., 2012), with the SILVA Ref NR 99 database version 119 as reference (available at <http://www.arb-silva.de/download/arb-files/>). FastTree (Price et al., 2010) was then used to build phylogenetic trees from the SINA alignments, using default settings.

### 3. Results

#### 3.1. Microcosm growth experiment

The microcosm experiment revealed that growth rate of microbial phototrophs in the Toklat Glacier's supraglacial soils is limited by P, but that the final % cover in the microcosms was co-limited by P and N (Fig. 1). Until day 34 of the microcosm

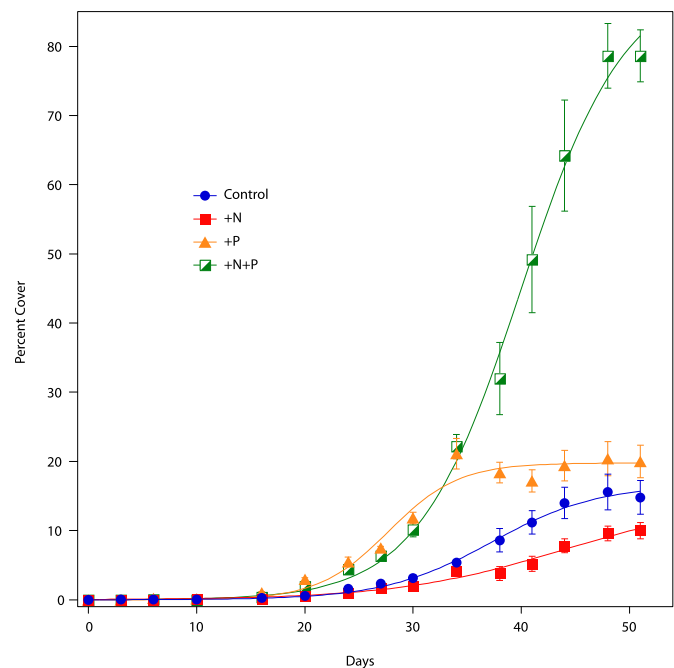


**Fig. 1. Growth curves for Toklat Glacier microcosms.** Each point is the mean of five replicate microcosms (error bars are standard error of the mean). Both the +N+P (green split rectangles) and the +P (orange triangles) treatments exhibited rapidly accelerating increases in percent cover. However, the +P treatment was quickly limited by a lack of N, as it plateaued at roughly 30 days. Both the control (blue circles) and the +N treatment (red squares) had a much slower acceleration of growth than the treatments that included P, and also had a much lower final percent coverage. The +N treatment had the lowest percent coverage, indicating that without added P, N inhibited growth of microbial phototrophs to some extent, however this pattern is not robust (Table 1). Data points from before day 34 were obtained via the FOV method (Schmidt et al., 2012) and were converted to percent cover estimates using our mathematical model (Supplemental Fig. 1). (For interpretation of the references to colour in this figure legend, the reader is referred to the web version of this article.)

experiment, +P and +N+P microcosms showed similar growth patterns, increasing in percent cover more rapidly (higher growth rate) than control or +N microcosms. However, after day 34, +N+P microcosms continued to grow, while growth in the +P microcosms plateaued. Thus, microbial phototrophs in +N+P microcosms attained total covers over four times higher than all other microcosms by the end of the experiment, and the other treatments and control plateaued with similar final percent cover values ( $K$ , Equation (2), Table 1). Therefore, both N and P significantly affected  $K$ , however the presence of a significant interaction term ( $P_{N:P}$ , Table 1) indicates that the effect of P or N is different when the other is present (as in the +N + P treatment). The other parameters in the logistic equation also responded to the addition of N and P, however only the ANOVA for  $K$  produced a significant interaction term. The logistic inflection point,  $i$ , responded significantly to both N and P. However, the exponential growth rate,  $r$ , was higher in treatments containing P (+P, +N+P) but was not significantly affected by N (Table 1).

### 3.2. Residual nitrogen biogeochemistry

Commensurate with +N microcosms exhibiting the slowest growth, these microcosms also contained the highest residual N levels (Fig. 3). +N microcosms contained concentrations of nitrate+nitrite roughly ten times higher than other treatments, but no significant differences were observed between other treatments ( $P_{+N/Control} = 0.027$ ,  $P_{+N/+P} = 0.025$ ,  $P_{+N/+N+P} = 0.026$ , Tukey's HSD). The mean ammonia concentration was also highest in the +N treatment (Fig. 2). However, no statistically significant difference in ammonia concentration was detected among the treatments.

### 3.3. Bacterial community analysis

High-throughput sequencing of the microcosms for all three domains of life revealed that bacterial and eukaryal communities were significantly changed by treatment (Fig. 3). Archaea were not detected at all, even though the bacterial primer set does amplify archaeal 16S rDNA. Archaeal sequences were detected in positive controls run in the same MiSeq lane using the same PCR reagents and the same thermocycler, indicating that their absence in the Toklat Glacier microcosm data set may be real (data not shown). ADONIS analysis of both data sets revealed significant effects of both N and P (for bacteria,  $P_N = 0.001$ ,  $P_P = 0.002$ ; for eukaryotes,  $P_N = 0.001$ ,  $P_P = 0.001$ ). Phylogenetic analysis of the microbial communities from each microcosm treatment revealed that photosynthetic bacteria were not highly abundant in any treatment, although photosynthetic eukaryotes dominated every microcosm's 18S rDNA library. Several bacterial OTUs were highly abundant across different treatments, such as an OTU which was abundant in the control and +P treatments, and was a close BLAST match to *Thiobacillus denitrificans*. Other abundant bacterial OTUs were related to *Lysobacter* (+P and +N+P), *Kaistobacter* (+N), an uncultured Acidobacterium (+P), *Fimbriimonas* (+N+P), and an

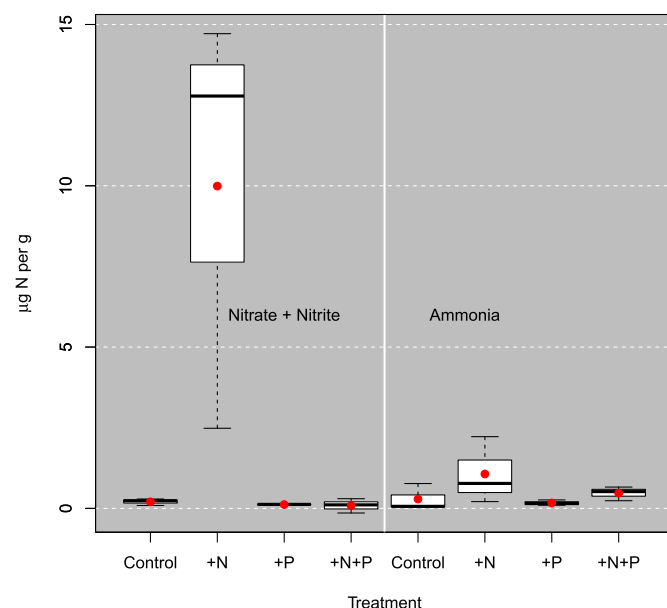


**Fig. 2. Residual inorganic nitrogen concentrations of microcosms.** +N microcosms had very high levels of residual inorganic N at the end of the experiment, presumably due to an inability to metabolize excess N without sufficient P. However, there was no excess N detectable in the +N+P treatment, indicating that added P enables N use. Red dots indicate the mean. (For interpretation of the references to colour in this figure legend, the reader is referred to the web version of this article.)

uncultured Planctomycete (control). The only cyanobacteria within the top 20 most abundant OTUs were from the control. One was an uncultured basal cyanobacterium, and the other was a close BLAST match to *Crinalium epipsammum*.

### 3.4. Eukaryal community analysis

Eukaryal OTUs were mainly algal, and *Bracteacoccus* spp. were the dominant OTUs in the non-control microcosms (Fig. 4). In the control microcosms, a moss in the Polytrichaceae was the dominant OTU, and it was also abundant (but not dominant) in the +N and +P treatments. Abundant algal OTUs were related to *Stichococcus*, *Characium*, and *Pseudendoconopsis*, the latter two of which have already been shown to inhabit the Toklat Glacier site (Schmidt and Darcy, 2014). Some heterotrophic eukaryotes were abundant as well, including the rotifer *Philodina* and the amoeba *Glaeseria*. Richness (number of OTUs) was lower in +N+P microcosms than it was in microcosms from other treatments, and phylodiversity was higher in +P microcosms than it was in other treatments (Fig. 5).

## 4. Discussion

Although we previously identified some of the organisms that live on the Toklat glacier, and speculated as to how they form a

**Table 1**

**Logistic growth model comparison.** This table shows the parameter estimates of logistic models fit to growth data from each microcosm, averaged by treatment. Numbers in parenthesis are standard deviations of  $n$  replicate microcosms. Only 4 of the 5 +N+P microcosms were used in these calculations because one microcosm did not plateau, so the logistic model estimated over 100% cover.  $P$ -values are shown in the rightmost 3 columns for the 2-way ANOVAs run for each parameter. Independent variables in the three ANOVAs were Boolean: N (true or false) and P (true or false). The significant interaction term for  $K$  indicates that asymptotic percent cover responded differently to P addition when N was added versus when N was not added (or vice-versa).

Parameter	"Control"	" +N"	" +P"	" +N+P"	$P_P$	$P_N$	$P_{N:P}$
$K$ (% cover)	16.7 (6.17)	14.0 (3.15)	20.1 (5.67)	88.4 (11.1)	$9.94 \times 10^{-9}$	$6.10 \times 10^{-8}$	$9.21 \times 10^{-9}$
$r$ ( $\text{days}^{-1}$ )	0.22 (0.62)	0.14 (0.22)	0.25 (0.06)	0.25 (0.07)	$9.17 \times 10^{-3}$	0.129	0.126
$i$ (days)	36.7 (2.50)	43.2 (3.10)	28.2 (2.34)	39.1 (2.80)	$5.37 \times 10^{-5}$	$5.35 \times 10^{-6}$	0.099
$n$	5	5	5	4	–	–	–

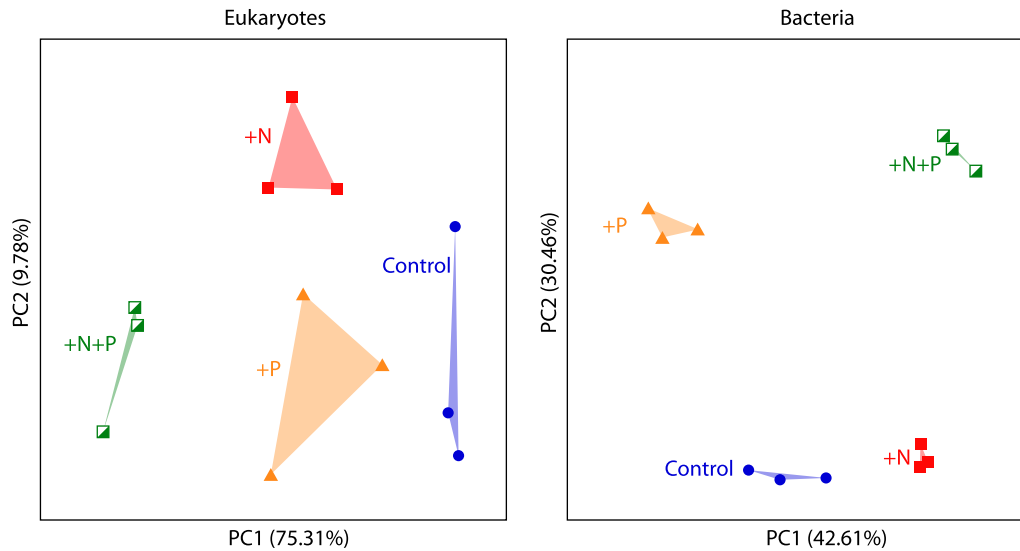


**Fig. 3.** Principle coordinates analysis of bacteria and eukaryotes from the microcosms. Both bacterial and eukaryal communities significantly responded to N and P addition, and communities from the same treatment were more similar to each other than they were to communities from other treatments. In the bacterial plot (right panel), PC1 corresponds to N addition, since the two communities that cluster on the left do not have added N and the two communities that cluster on the right do have added N. Similarly, PC2 corresponds to P addition, since the two communities on the bottom do not have added P and the two on the top do. The eukaryal community also segregated based on the treatment, but the interpretation of the principal coordinate axes is not so straightforward. Nevertheless, each treatment resulted in a unique microbial community of eukaryotes.

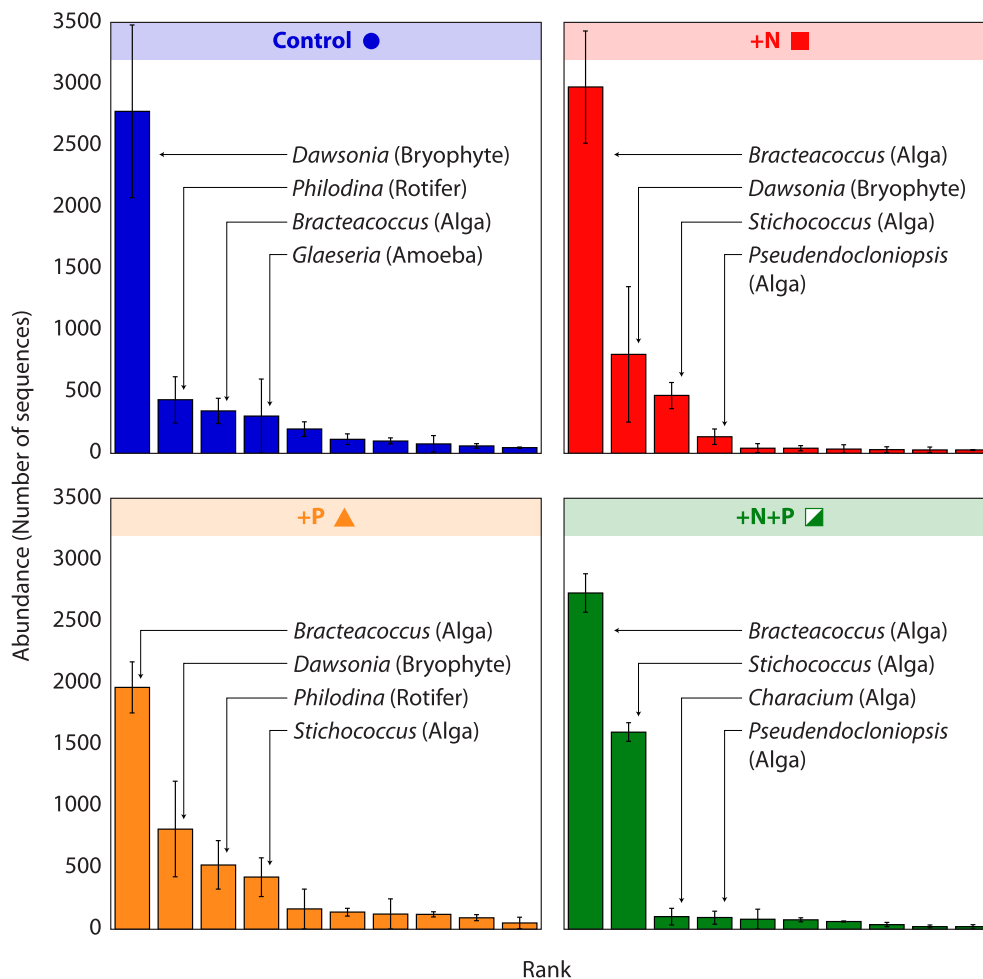


**Fig. 4.** Rank-abundance plots of eukaryal OTUs by treatment. In all treatments except the control (blue), *Bracteacoccus* dominated the eukaryal community. In the control treatment, a moss, *Dawsonia*, was the most abundant OTU. Algae closely related to the genus *Pseudendoconionopsis* have been previously detected in the same supraglacial debris that were used to make the microcosms discussed here (Schmidt and Darcy, 2014), however they are much less proportionally represented in the microcosm communities than they were *in situ*. (For interpretation of the references to colour in this figure legend, the reader is referred to the web version of this article.)

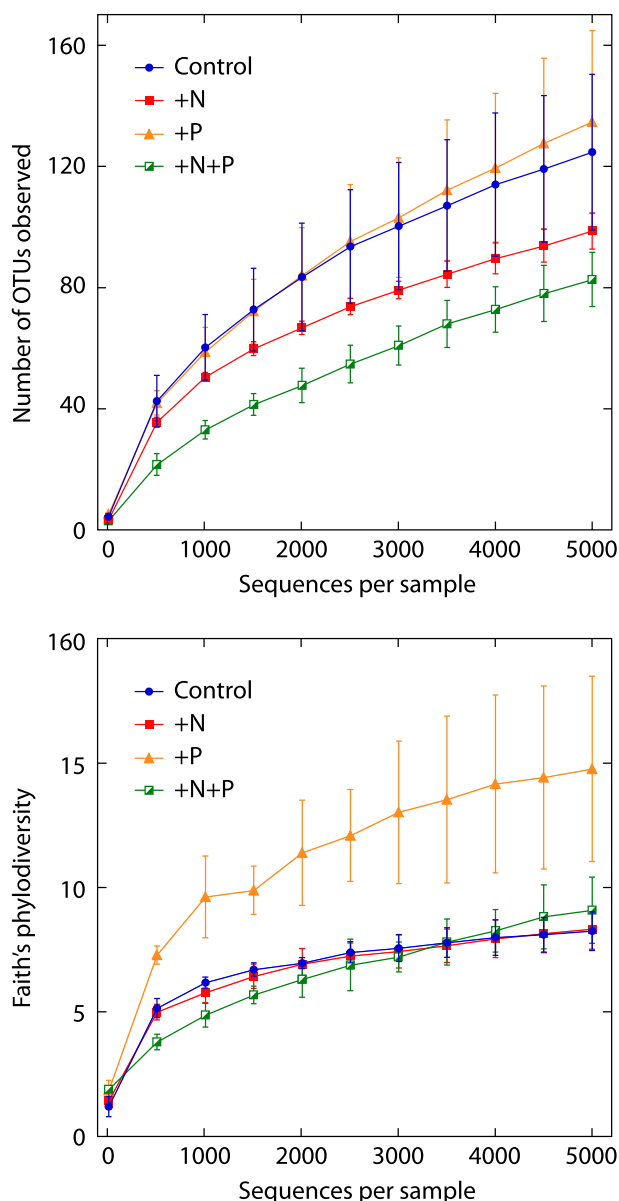


**Fig. 5. Alpha rarefaction for eukaryal communities.** Alpha rarefaction using the OTUs observed metric (also called “species observed”) showed that fewer OTUs were present in +N+P microcosms (top panel). Faith's (1992) phylogenetic diversity (bottom panel) is a different alpha-diversity metric, which sums branch lengths of divergent OTUs, meaning that the calculated value is indicative of how many deeply divergent taxa are present at a given sampling depth. This metric reveals that P addition increased phylogenetic diversity relative to the other three treatments. While OTUs observed do not saturate with increased resampling size, Faith's (1992) phylogenetic diversity does, indicating that the lack of saturation in the first metric is due to incomplete sampling of OTUs that are phylogenetically similar to those already detected.

simple, low-diversity community (Darcy et al., 2011; Schmidt and Darcy, 2014), phylogenetic data alone do not lend themselves to mechanistic explanations of which factors limit phototrophic growth in this unique environment. To this end, the present study showed that P limited the growth rate whereas P and N limited the final percent cover in these soils (Fig. 1). Several other studies have examined nutrient limitations of microbial phototrophs in arctic and alpine environments, but none so far have studied debris-covered glaciers. Furthermore, there have been only three previous studies of the indigenous microbiota of supraglacial debris (Darcy et al., 2011; Franzetti et al., 2013; Schmidt and Darcy, 2014).

However, studies of similar environments indicate that P may limit growth. For example, analysis of cryoconite on the Svalbard Glacier indicated that P may be limiting (Stibal et al., 2009) and microcosm studies similar to those done here showed that P limited both the growth rate and percent cover of phototrophic communities near the retreating Puca glacier in the Peruvian Andes (Schmidt et al., 2012). An *in-situ* fertilization experiment at the same site showed that co-addition of N and P accelerated the succession of the microbial community leading to a significant increase in phototrophic microbes (Knelman et al., 2014).

Similar to the abovementioned studies of nutrient limitation in the cryosphere, our results show P as the principally limiting nutrient (Fig. 1). P-addition significantly accelerated growth rate (Table 1), which is especially evident between days 20 through 34 of the microcosm experiment (Fig. 1). Had we stopped the microcosm experiment at day 34, we would have observed a clear pattern of P limitation even for percent cover. However at later time points, +N+P microcosms outpaced the other treatments by a large margin. The final percent cover estimates ( $K$  values, Equation (2)) overlapped to a large extent for all treatments except +N+P (Table 1), and the final cover for +N+P treatments was greater than the sum of control, +N and +P treatments. This non-additive result has been previously described as “Synergistic Co-limitation” (Allgeier et al., 2011). In synergistic co-limitation, the effect of the +N+P treatment is greater than the effects of +N added to +P, which is what we observed (Fig. 1, Table 1). This result is similar to results from many aquatic systems, but differs from most terrestrial systems, including Arctic systems, where an antagonistic response is usually observed (Allgeier et al., 2011). But although we observed N/P co-limitation of final percent cover, it is clear that P-limitation occurred before N limitation, so we characterize the microcosms as principally P-limited.

The  $K$  parameter in our logistic model represents percent cover values used in other full-factorial N and P addition studies (Elser et al., 2007; Harpole et al., 2011), but the growth rates we report ( $r$ , equation (2)) have not been measured in many previous studies. Had we not collected time-series data on this experiment, we would only have observed the end effect, and concluded that the system is synergistically co-limited by N and P. However thanks to the resolution of our time series, we observed that growth rate of microbial phototrophs is P-limited. Furthermore, from the inflection point parameter ( $i$ , equation (2)) we observed that +N microcosms took the longest to reach their peak instantaneous growth rate (*i.e.* change in % cover gained per day), but +P microcosms reached their peak instantaneous growth rate the fastest, over two weeks earlier than +N microcosms. The slow growth of +N microcosms is commensurate with the inorganic nitrogen data we collected, which clearly show that added N was not fully utilized unless P was also added (Fig. 2). The +N+P microcosms received the same amount of ammonium nitrate as the +N microcosms, but presumably due to a lack of P, the +N microcosms were not able to use the added N. Although they did not measure inorganic N concentration after their microcosm experiment, Schmidt et al. (2012) observed that N addition alone resulted in microcosms that grew less than the control, and at a slower growth rate than microcosms with added P.

Unlike the patterns of percent cover and residual inorganic N where a single treatment was highly different than the rest, the microbial communities of all four microcosm treatments were distinct from each other, and all were significantly affected by both N and P (Fig. 3). This result suggests that the mechanism by which nutrient addition affected growth (Fig. 1) was not simply an effect that caused more of the same organisms to grow, but rather that the treatments selected for the growth of different organisms (Fig. 3). Even when total growth (in terms of percent cover) was not

dramatically affected, as was the case between the control, +N, and +P microcosm treatments, different microbial communities developed indicating strongly deterministic selection (Nemergut et al., 2013) by each nutrient regime. In addition, the bacterial communities of the microcosms were very diverse, with no OTU composing more than 4% of the 16S amplicon libraries from control microcosms, and no OTU composing more than 9% of any other microcosm. Among the most common bacteria that grew in the microcosms without added N were *Thiobacillus*, which have been detected before in other periglacial environments, such as beneath the Bench glacier (Skidmore et al., 2005), which is also in Alaska although it is roughly 342 km from the Toklat glacier. In treatments containing added P (+P and +N+P), an OTU assigned to the genus *Lysobacter* was highly abundant, which may be a denizen of the rhizosphere (Hayward et al., 2010). However, for such an inconspicuous genus it is difficult to generalize traits based on a ~250 bp 16S rDNA sequence. Even the ecological role of one cyanobacterial OTU (ML635J-21) detected within the microcosms is not easily understood. ML635J-21 was only detected in the control microcosms, where it was the most abundant OTU in one microcosm, and is the most basal clade in the Cyanobacteria, has no cultured representatives, and may not even be phototrophic since many phylogenotypes come from aphotic environments (Soo et al., 2014). The only other cyanobacterium we detected was a close match to *Crinallium*. This cyanobacterium is definitely phototrophic, and the genus *Crinallium* has been detected in Antarctic glacial cryoconite (Broadly and Kibblewhite, 1991; Mueller and Pollard, 2004; Porzinska et al., 2004).

Unlike the bacteria, the eukaryotes we sequenced were almost entirely phototrophic (Fig. 4). In every microcosm except the controls, an OTU from the algal genus *Bracteacoccus* dominated. *Bracteacoccus* have been isolated from cryoconite holes, but also from supraglacial debris (Stibal et al., 2006). These algae were also observed by Kaštovská et al. (2005) in barren glacial soils, but not in vegetated soils nearby. Commensurate with our observations, Shukla et al. (2011) found that out of 6 algal isolates from recently deglaciated soil, only *Bracteacoccus* responded well to excess N. However, this N copiotrophy does not explain why *Bracteacoccus* still dominate the 18S libraries for +P microcosms, where no N was added. These algae were not the dominant OTU in the control microcosms, and we found a bryophyte OTU to be most abundant instead. The two different classification methods we used disagreed on the genus of this OTU, returning closely related genera *Dawsonia* (SINA) or *Notoligotrichum* (BLAST) both of which are in the family Polytrichaceae (Bell and Hyvonen, 2012). Whatever the exact identity of this moss OTU, it was clearly selected against by any nutrient addition. Similarly, Schmidt et al. (2012) found that mosses were inhibited by all nutrient addition treatments and they speculated that these mosses could be adapted to oligotrophic conditions, and our observations support this hypothesis because of the dominance of putatively copiotrophic *Bracteacoccus* algae in nutrient addition microcosms.

Our phylogenetic comparisons also show that the excess growth of phototrophs in the +N+P treatment was likely due to the growth of a few dominant organisms, because the total number of OTUs detected was reduced by this treatment (Fig. 5, top panel). Similar to the pattern observed with final percent cover estimates, control, +N, and +P microcosms overlap in the number of OTUs observed during alpha rarefaction, while the +N+P microcosms had lower richness. However, when a metric such as Faith's Phylodiversity (Faith, 1992) is used instead of the number of observed OTUs, a different pattern emerges in which +P microcosms contain significantly more phylodiversity than the other three treatments (Fig. 5, bottom panel). Faith's phylodiversity is an alpha diversity metric that uses phylogenetic distance instead of OTU counts, so

that closely related OTUs (which have low phylogenetic distance) are less important to the output than distantly related OTUs. This means that the +P microcosms contain more distantly related eukaryal OTUs than other microcosms, indicating that P allowed the growth of a broader diversity of organisms than did the other treatments.

Taken together, the results of our molecular, physiological, and biogeochemical studies form a preliminary picture of how low nutrient levels might limit life atop the Middle Fork Toklat Glacier, and perhaps other debris-covered glaciers. Our microcosm results suggest that the growth rate of microbial phototrophs on the Toklat Glacier is P-limited, but total growth (final percent cover) may be co-limited by N and P. Our results also suggest that N and P differentially stimulate members of the indigenous microbiome resulting in the formation of different microbial communities in response to each treatment. Future work will be focused on understanding the growth strategies of these individual taxa to better understand how they may respond to future inputs of nutrients either due to continued successional processes or anthropogenic inputs of nutrients.

#### Data accessibility

Sequence data and associated metadata from this study have been deposited in FigShare and are available with the DOI <http://dx.doi.org/10.6084/m9.figshare.1427427>.

#### Acknowledgments

We thank B.T. Todd and W.A. Schrepel for laboratory assistance and A.J. King, B.-L. Conciencie and M. Mitter for collecting the soils used in this study. Funding was provided by NSF grants for studying microbial community assembly (DEB-1258160), and the LTER program (DEB-1027341) and the USAF Office of Scientific Research (FA9550-14-1-0006).

#### Appendix A. Supplementary data

Supplementary data related to this article can be found at <http://dx.doi.org/10.1016/j.soilbio.2015.12.019>.

#### References

- Allgeier, J.E., Rosemond, A.D., Layman, C.A., 2011. The frequency and magnitude of non-additive responses to multiple nutrient enrichment. *Journal of Applied Ecology* 48, 96–101.
- Altschul, S.F., Gish, W., Miller, W., Myers, E.W., Lipman, D.J., 1990. Basic local alignment search tool. *Journal of Molecular Biology* 215, 403–410.
- Amaral-Zettler, L.A., McCliment, E.A., Ducklow, H.W., Huse, S.M., 2009. A method for studying protistan diversity using massively parallel sequencing of V9 hyper-variable regions of small-subunit ribosomal RNA genes. *PLoS One* 4, e6372.
- Bell, N., Hyvonen, J., 2012. Gametophytic simplicity in Laurasian and Gondwanan Polytrichopsida — the phylogeny and taxonomy of the Oligotrichum morphology. *Journal of Bryology* 34, 160–172.
- Belnap, J., Lange, O.L., 2001. Structure and function of biological soil crusts: synthesis. In: Belnap, J., Lange, O.L. (Eds.), *Biological Soil Crusts: Structure, Function, and Management*. Springer, Berlin, pp. 471–480.
- Broadly, P.A., Kibblewhite, A.L., 1991. Morphological characterization of Oscillatoriales (Cyanobacteria) from Ross Island and southern Victoria Land, Antarctica. *Antarctic Science* 3, 35–45.
- Caporaso, J.G., Kuczynski, J., Stombaugh, J., Bittinger, K., Bushman, F.D., Costello, E.K., Fierer, N., Peña, A.G., Goodrich, J.K., Gordon, J.I., Huttley, G.A., Kelley, S.T., Knights, D., Koeng, J.E., Ley, R.E., Lozupone, C.A., McDonald, D., Muegge, B.D., Pirrung, M., Reeder, J., Sevinsky, J.R., Turnbaugh, P.J., Walters, W.A., Widmann, J., Yatsunenko, T., Zaneveld, J., Knight, R., 2010. QIIME allows analysis of high-throughput community sequencing data. *Nature Methods* 7, 335–336.
- Caporaso, J.G., Lauber, C.L., Walters, W.A., Berg-Lyons, D., Huntley, J., Fierer, N., Owens, S.M., Betley, J., Frasset, L., Bauer, M., Gormley, N., Gilbert, J.A., Smith, G., Knight, R., 2012. Ultra-high-throughput microbial community analysis on the Illumina HiSeq and MiSeq platforms. *ISME* 6, 1621–1624.

- Cleveland, C.C., Liptzin, D., 2007. C:N:P stoichiometry in soil: is there a "Redfield ratio" for the microbial biomass? *Biogeochemistry* 85, 235–252.
- Darcy, J.L., Lynch, R.C., King, A.J., Robeson, M.S., Schmidt, S.K., 2011. Global distribution of *Polaromonas* phylotypes - evidence for a highly successful dispersal capacity. *PLoS One* 6, e23742.
- Edgar, R.C., 2010. Search and clustering orders of magnitude faster than BLAST. *Bioinformatics* 26, 2460–2461.
- Elser, J.J., Bracken, M.E.S., Cleland, E.E., Gruner, D.S., Harpole, W.S., Hillebrand, H.H., Nagi, J.T., Seabloom, E.W., Shurin, J.B., Smith, J.E., 2007. Global analysis of nitrogen and phosphorus limitation of primary producers in freshwater, marine and terrestrial ecosystems. *Ecology Letters* 10, 1135–1142.
- Faith, D.P., 1992. Conservation evaluation and phylogenetic diversity. *Biological Conservation* 61, 1–10.
- Fenn, M.E., Haeuber, R., Tonnesen, G.S., Baron, J.S., Grossman-Clarke, S., Hope, D., Jaffe, D.A., Copeland, S., Geiser, L., Rueth, H.M., Sickman, J.O., 2003. Nitrogen emissions, deposition, and monitoring in the western United States. *BioScience* 53, 391–403.
- Franzetti, A., Tatangelo, V., Gandolfi, I., Bertolini, V., Bestetti, G., Diolaiuti, G., D'Agata, C., Mihalcea, C., Smiraglia, C., Ambrosini, R., 2013. Bacterial community structure on two alpine debris-covered glaciers and biogeography of *Polaromonas* phylotypes. *ISME* 7, 1483–1492.
- Göransson, H., Venterink, H.O., Bååth, E., 2011. Soil bacterial growth and nutrient limitation along a chronosequence from a glacier forefield. *Soil Biology & Biochemistry* 43, 1333–1340.
- Harpole, W.S., Ngai, J.T., Cleland, E.E., Seabloom, E.W., Borer, E.T., Bracken, M.E.S., Elser, J.J., Gruner, D.S., Hillebrand, H., Shurin, J.B., Smith, J.E., 2011. Nutrient co-limitation of primary producer communities. *Ecology Letters* 14, 852–862.
- Hayward, A.C., Fegan, N., Fegan, M., Stirling, G.R., 2010. *Stenotrophomonas* and *Lysobacter*: ubiquitous plant-associated gamma-proteobacteria of developing significance in applied microbiology. *Journal of Applied Microbiology* 108, 756–770.
- Kaštovská, K., Elster, J., Stibal, M., Šantrůčková, H., 2005. Microbial assemblages in soil microbial succession after glacial retreat in Svalbard (High Arctic). *Microbial Ecology* 50, 396–407.
- King, A.J., Meyer, A.F., Schmidt, S.K., 2008. High levels of microbial biomass and activity in unvegetated tropical and temperate alpine soils. *Soil Biology & Biochemistry* 40, 2605–2610.
- Knelman, J.E., Schmidt, S.K., Lynch, R.C., Darcy, J.L., Castle, S.C., Cleveland, C.C., Nemergut, D.R., 2014. Nutrient addition dramatically accelerates microbial community succession. *PLoS One* 9, e102609.
- Lozupone, C., Knight, R., 2005. UniFrac: a new phylogenetic method for comparing microbial communities. *Applied and Environmental Microbiology* 71, 8228–8235.
- Mueller, D.R., Pollard, W.H., 2004. Gradient analysis of cryoconite ecosystems from two polar glaciers. *Polar Biology* 27, 66–74.
- Nakawo, M., Raymond, C.F., Fountain, A. (Eds.), 2000. *Debris-Covered Glaciers*. International Association of Hydrological Sciences Press, Oxfordshire UK.
- Nemergut, D.R., Schmidt, S.K., Fukami, T., O'Neill, S.P., Billinski, T.M., Stanish, L.F., Knelman, J.E., Darcy, J.L., Lynch, R.C., Wickey, P., Ferrenberg, S., 2013. Patterns and processes of microbial community assembly. *Microbiology and Molecular Biology Reviews* 77, 342–356.
- Nemergut, D.R., Anderson, S.P., Cleveland, C.C., Martin, A.P., Miller, A.E., Seimon, A., Schmidt, S.K., 2007. Microbial community succession in unvegetated, recently-deglaciated soils. *Microbial Ecology* 53, 110–122.
- Oksanen, J., Blanchet, F.G., Kindt, R., Legendre, P., Minchin, P.R., O'Hara, R.B., Simpson, G.L., Solymos, P., Stevens, M.H.H., Wagner, H., 2013. *Vegan: Community Ecology Package*. R Package Version 2.0-10. <http://CRAN.R-project.org/package=vegan>.
- Porazinska, D.L., Fountain, A.G., Nylen, T.H., Tranter, M., Virginia, R.A., Wall, D.H., 2004. The biodiversity and biogeochemistry of cryoconite holes from McMurdo dry valley glaciers, Antarctica. *Arctic, Antarctic, and Alpine Research* 36, 84–91.
- Price, M.N., Dehal, P.S., Arkin, A.P., 2010. FastTree 2 – approximately maximum-likelihood trees for large alignments. *PLoS One* 5, e9490.
- Preusse, E., Peplies, J., Glöckner, O., 2012. SINA: accurate high-throughput multiple sequence alignment of ribosomal RNA genes. *Bioinformatics* 14, 1823–1829.
- R Core Team, 2013. *R: a Language and Environment for Statistical Computing*. R Foundation for Statistical Computing, Austria, Vienna. <http://www.R-project.org/>.
- Scherler, D.B., Bookhagen, B., Strecker, M.R., 2011. Spatially variable response of Himalayan glaciers to climate change affected by debris cover. *Nature Geosciences* 4, 156–159.
- Schmidt, S.K., Darcy, J.L., 2014. Phylogeography of ulotrichalean algae from extreme high-altitude and high-latitude ecosystems. *Polar Biology*. <http://dx.doi.org/10.1007/s00300-014-1631-6>.
- Schmidt, S.K., Nemergut, D.R., Todd, B.T., Lynch, R.C., Darcy, J.L., Cleveland, C.C., King, A.J., 2012. A simple method for determining limiting nutrients for photosynthetic crusts. *Plant Ecology & Diversity* 5, 513–519.
- Schmidt, S.K., Lynch, R.C., King, A.J., Karki, D., Robeson, M.S., Nagy, L., Williams, M.W., Mitter, M.S., Freeman, K.R., 2011a. Phylogeography of microbial phototrophs in the dry valleys of the high Himalayas and Antarctica. *Proceedings of the Royal Society Biology* 278, 702–708.
- Schmidt, S.K., Cleveland, C.C., Nemergut, D.R., Reed, S.C., King, A.J., Sowell, P., 2011b. Estimating phosphorus availability for microbial growth in an emerging landscape. *Geoderma* 163, 135–140.
- Shukla, P.S., Kvidrová, J., Elster, J., 2011. Nutrient requirements of polar *Chlorella*-like species. *Czech Polar Reports* 1 (1), 10.
- Skidmore, M., Anderson, S.P., Sharp, M., Foght, J., Lanoil, B.D., 2005. Comparison of microbial community compositions of two subglacial environments reveals a possible role for microbes in chemical weathering processes. *Applied and Environmental Microbiology* 71, 6986–6997.
- Soo, R.M., Skennerton, C.T., Sekiguchi, Y., Imelfort, M., Paech, S.J., Dennis, P.G., Steen, J.A., Parks, D.H., Tyson, G.W., Hugenholtz, P., 2014. An expanded genomic representation of the phylum cyanobacteria. *Genome Biology and Evolution* 6, 1031–1045.
- Stibal, M., Šabacká, M., Kaštovská, K., 2006. Microbial communities on glacier surfaces in Svalbard: impact of physical and chemical properties on abundance and structure of cyanobacteria and algae. *Microbial Ecology* 52, 644–654.
- Stibal, M., Anesio, A.M., Blues, C.J.D., Tranter, M., 2009. Phosphatase activity and organic phosphorus turnover on a high Arctic glacier. *Biogeosciences* 6, 913–922.